Available online at www.sciencedirect.com
SCIENCE DIRECT®
C. R. Chimie 7 (2004) 1141–1152
COMPTES RENDUS CHIMIE
http://france.elsevier.com/direct/CRAS2C/

Full paper / Mémoire

Immobilisation of actinides in phosphate matrices

Nicolas Dacheux [a,*], Nicolas Clavier [a], Anne-Charlotte Robisson [a], Olivier Terra [a], Fabienne Audubert [b], Jean-Éric Lartigue [b], Christophe Guy [b]

[a] *Groupe de radiochimie, Institut de physique nucléaire, bât. 100, université de Paris-Sud (Paris-11), 91406 Orsay, France*
[b] *DEN/DED/SEP/LCC, CEA Cadarache, BP 108, 13108 St Paul-lez-Durance, France*

Received 15 September 2003; accepted after revision 2 February 2004

Available online 13 October 2004

Abstract

In the field of the immobilisation of high-activity-level and long-life radwaste (HAVL) for a deep underground repository, several phosphate matrices were already proposed as good candidates to delay the release of actinides in the near-field of such disposal. Among them, thorium phosphate–diphosphate (TPD), monazites/brabantites, britholites, and TPD/monazite composites were extensively studied. The synthesis of samples doped with actinides (Th, U...) through wet and dry chemistry methods then their complete characterisation are reported. Their chemical durability is also examined. These materials appear as promising matrices to immobilise tetravalent and/or trivalent actinides. ***To cite this article: N. Dacheux et al., C. R. Chimie 7 (2004).***

Résumé

Immobilisation des actinides dans des matrices phosphatées. Dans l'optique d'un stockage de déchets radioactifs de haute activité et de vie longue en site géologique profond, plusieurs matrices phosphatées de type céramique ont été proposées afin de retarder le relâchement des actinides dans le champ proche d'un tel stockage. Parmi celles-ci, le phosphate-diphosphate de thorium (PDT), les monazites, les brabantites et les britholites présentent plusieurs des propriétés recherchées pour assurer la rétention de ces éléments sur le long terme. La préparation d'échantillons dopés avec des actinides par voie sèche et/ou humide, leur caractérisation à l'état pulvérulent ou fritté et leur durabilité chimique lors de tests de lixiviation sont examinées ici. Sur la base des propriétés physico-chimiques de ces matrices, des matériaux composites à base de PDT et de monazite ont été préparés puis caractérisés. Tous ces matériaux apparaissent comme des candidats prometteurs pour l'immobilisation des actinides tri- et tétravalents. ***Pour citer cet article : N. Dacheux et al., C. R. Chimie 7 (2004).***

Keywords: Actinides immobilisation; Ceramic matrices; Phosphate; Sintering; Radwaste storage

Mots clés : Immobilisation des actinides ; Matrices céramiques ; Phosphate ; Frittage ; Stockage des déchets radioactifs

* Corresponding author.
E-mail address: dacheux@ipno.in2p3.fr (N. Dacheux).

1631-0748/$ - see front matter © 2004 Académie des sciences. Published by Elsevier SAS. All rights reserved.
doi:10.1016/j.crci.2004.02.019

1. Introduction

Considering several interesting properties, phosphate matrices like apatites $Ca_{10}(PO_4)_6F_2$ [1] and britholites $Ca_9Nd(PO_4)_5(SiO_4)F_2$ [2], monazites $M^{III}PO_4$ [3,4] and brabantites $M^{II}M^{IV}(PO_4)_2$ [5–7], sodium–zirconium phosphate $NaZr_2(PO_4)_3$ (NZP) [8,9], zirconium phosphates like $Zr_2O(PO_4)_2$ [10] or thorium phosphates like $Th_4(PO_4)_4P_2O_7$ (TPD) [11] could be potential candidates for the immobilisation of actinides coming from an advanced reprocessing of spent fuel or for the final disposal of the excess plutonium from dismantled nuclear weapons. Indeed, phosphate materials and minerals are generally considered to be very low soluble (we can report for instance, the good retention of thorium and uranium in several phosphate ores containing monazites, brabantites or apatites). Moreover, these minerals appear generally to be resistant to radiation damages (for example, we can report on the existence of crystallized monazites containing up to 30 wt% of thorium in the structure) [3,12].

However, the literature of actinide phosphates was rather poor and often controversial. In these conditions, the chemistry of uranium and thorium phosphates [13–17] was completely re-examined since few years. Several compounds were characterized in the ThO_2-P_2O_5 and UO_2-P_2O_5 systems. Among these materials, the uranium–uranyl phosphate $U(UO_2)(PO_4)_2$, the diuranium oxide phosphate $U_2O(PO_4)_2$ and the thorium phosphate-diphosphate ($Th_4(PO_4)_4P_2O_7$ or $Th_4P_6O_{23}$, namely TPD) were prepared as pure and well-crystallized phases [11,13,14]. In this paper, we will discuss about the immobilisation of tri- and tetravalent actinides in several phosphate matrices such as TPD, monazite, TPD/monazite composites, and britholites. For all the syntheses involving radionuclides of high specific activity, the experiments were achieved in glove box.

2. Thorium phosphate-diphosphate (TPD)

2.1. Preparation and characterisation

Several reasons led us to propose TPD (which does not present any natural analogue) for the immobilisation of tetravalent actinides like uranium, neptunium, and plutonium. First, Th^{4+} is the largest tetravalent cation of the periodic table: its ionic radius in the eight-fold coordination being equal to 1.05 Å, it could be easily replaced by one of the other smaller tetravalent actinides ($^{VIII}r_{cat.}$ equal to 1.00 Å, 0.98 Å and 0.96 Å for uranium, neptunium and plutonium, respectively) [18]. This material is easy to prepare in the powder and in the pellet form and is highly resistant to aqueous alteration. Finally, the low-soluble phases precipitated in the back-end of the initial dissolution step should delay significantly the release of actinides in a deep underground disposal storage and consequently their migration to the biosphere.

Various ways of preparation of few grams of TPD and associated solid solutions using either wet and dry chemistry methods were already reported [11,17,19]. Among these ways, we prefer its preparation from a mixture of concentrated solutions containing thorium nitrate or chloride (0.5–2 M), the given tetravalent actinide (U, Np, Pu, which solutions were prepared from metal or oxides) and 5M phosphoric acid in order to increase the homogeneity of the final samples. The mixtures prepared considering the mole ratio $(Th + An^{IV})/PO_4 = 2/3$ are evaporated until dry residues are obtained. These solids are ground manually in ethanol, heated at 673 K for 2 h in order to perform the elimination of volatile products, then at 1323–1523 K for 10 to 18 h in order to obtain well-crystallized, homogeneous and single-phase samples. Several samples of $Th_{4-x}U_xP_6O_{23}$ (TUPD), $Th_{4-x}Np_xP_6O_{23}$ (TNpPD) and $Th_{4-x}Pu_xP_6O_{23}$ (TPuPD) solid solutions were synthesised with various compositions in concentrated hydrochloric media for TUPD solid solutions (in order to avoid the oxidation of tetravalent uranium into uranyl during the evaporation step) and in nitric acid for TNpPD and TPuPD solid solutions [20–23]. The chemical composition and purity of the samples (pure TPD or TUPD solid solutions) can be verified using Electron Probe MicroAnalyses (EPMA) and Particle-Induced X-ray Emission (PIXE) experiments [23]. The complete characterisation is based on XRD, IR and UV-Visible spectroscopies, etc., while the observations are performed using Scanning and Transmission Electron Microscopies.

The structure determination on powder and single crystal led to an orthorhombic unit cell for pure TPD (space group *Pcam*, $Z = 2$) with $a = 12.8646(9)$ Å, $b = 10.4374(8)$ Å and $c = 7.0676(5)$ Å ($V = 949.0(1)$ Å^3) [11]. The thorium environment in the TPD structure is

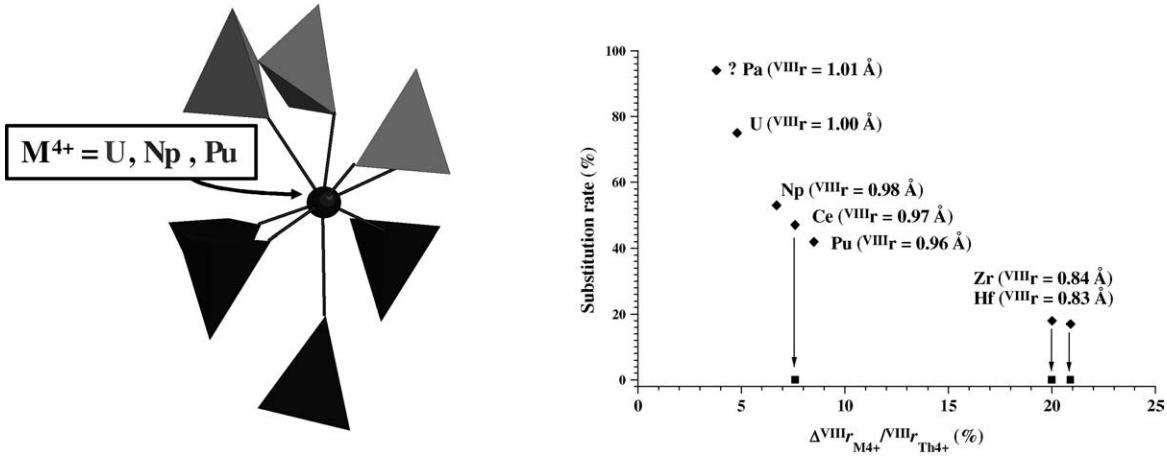

Fig. 1. Substitution of thorium in TPD. Representation of Th-environment showing one bidendate P_2O_7, one bidentate PO_4, and four monodentate PO_4 (left). Expected (♦) and experimental (■) substitution of thorium by tetravalent cation (right). For protactinium, only expected value because of high specific activity.

presented in Fig. 1. The replacement of thorium by other tetravalent actinides is followed by XRD. For each actinide studied (U, Np, Pu), the unit-cell parameters and volume decrease linearly when increasing the substitution rate of thorium, x, in the structure, as follows:

$$V_{\mathrm{TUPD}} = 949.0(6) - 10.0(4)x_U \quad (1)$$

$$V_{\mathrm{TNpPD}} = 947.9(9) - 14.4(9)x_{Np} \quad (2)$$

$$V_{\mathrm{TPuPD}} = 949.0(1) - 19.0(1)x_{Pu} \quad (3)$$

The thorium substitution appears possible up to 75 mol% (47.6 wt%) by U(IV), 52 mol% (33.2 wt%) by Np(IV) and 41 mol% (26.1 wt%) by Pu(IV). For higher substitution rates, polyphase systems are obtained. Attempts to synthesize pure $M_4(PO_4)_4P_2O_7$ (M = U, Np or Pu) lead always to polyphase systems (Table 1). Moreover, the preparation of pure $M_4(PO_4)_4P_2O_7$ (M = Zr, Hf or Ce) are unsuccessful too, probably because of the too small ionic radii of M^{4+} ions (0.84 and 0.83 Å for Zr and Hf, respectively) compared to that of thorium or of the redox properties (cerium (IV) being reduced during the heating treatment at high temperature, even in oxidizing conditions).

2.2. Sintering

In order to prepare densified pellets, the specific surface area (SA) of various compositions of powdered samples of TUPD solid solutions was followed versus the heating temperature. For $\theta \geq 1273$ K, we observe the significant decrease of the SA value due to the TUPD (or TPD) crystallization and to the increase of the grain size. It is correlated with the disappearance of the grain size population at 0.1–0.3 μm. The SA value of the powders prepared between 1373 and 1523 K reaches 0.2 to 3 m^2g^{-1} and the corresponding average grain size is found between 5 and 20 μm. Some agglomerates of 40–70 μm are also observed.

Sintered samples (shaped in rectangular or cylindrical forms) are currently obtained from a dry residue prepared after the slow evaporation of a mixture of concentrated solutions through a rather simple procedure based on two steps: uniaxial pressing at room temperature at 100–800 MPa, then heating at 1523 K for 2–10 h. For all the samples, the apparent relative density measured is found between 90 and 95% of the value calculated from XRD data, while the effective relative density usually reaches 94 to 99% [24]. Se-

Table 1
Systems obtained for $M^{IV}/PO_4 = 2/3$ (M=Zr, Hf, Ce, U, Np and Pu) in order to prepare $M_4(PO_4)_4P_2O_7$

M^{IV}	System obtained (1323–1523 K)
Zr	α-$ZrP_2O_7 + Zr_2O(PO_4)_2$
Hf	$Hf_{0.25}Hf_2(PO_4)_3 + Hf_2P_2O_9 + HfO_2$
Ce	α-$CeP_2O_7 + CePO_4$
U	α-$UP_2O_7 + U_2O(PO_4)_2$ (argon)
	α-$UP_2O_7 + U(UO_2)(PO_4)_2$ (air)
Np	α-$NpP_2O_7 + Np_2O(PO_4)_2$
Pu	α-$PuP_2O_7 + PuPO_4$

veral properties of TPD and/or TUPD pellets are gathered in Table 2 while micrographs of the surface and inside of a sintered TUPD ceramic (θ = 1523 K, t = 2.5 h) are presented in Fig. 2.

2.3. Chemical durability

The behaviour of TPD during leaching tests was examined by varying several parameters such as the surface (BET)/volume ratio (*S/V*), the temperature, the acidity or the basicity of the leachate, the leaching flow, the ionic strength and the phosphate concentration in the leachate [25–27]. As this material is very insoluble, some experiments are also performed in aggressive conditions (like 5 M and 10^{-1} M HNO_3) in order to increase the normalized dissolution rate (expressed in g m^{-2} d^{-1}). The kinetics is examined for low *S/V* ratios (25–692 cm^{-1}), while the neoformed phases are studied for higher *S/V* values when the saturation of the leachate is reached (through thermodynamic equilibriums).

Table 2
Physicochemical properties of TPD/TUPD ceramics [24]

Surface area (powder)	0.2 m^2 g^{-1}
Surface area (pellet)	600–1200 cm^2 g^{-1}
Average grain size	5–20 µm
$d_{app.}/d_{calc.}$	90–95%
$d_{eff.}/d_{calc.}$	94–99%
Open porosity	2–5%
Closed porosity	1–5%
Pore dimensions	Cylindrical : $\varnothing \approx 1$ µm ; $L \approx 2$ µm
Hardness	350–500 Hv
EPMA and PIXE	Homogeneous – Single phase

The dissolution of TPD doped or not with trivalent actinides (Am, Cm present at the tracer scale) and of TUPD or TPuPD solid solutions was studied from a kinetic point of view versus the acidity and the basicity of the leachate. At room temperature, the normalized dissolution rates are found between 1.2×10^{-5} and 4.4×10^{-9} g m^{-2} d^{-1}, which confirms the very good resistance of TPD and associated solid solutions to aqueous alteration.

The partial orders related to the proton (n) and to the hydroxide ion (m) concentrations reach 0.31–0.35 and 0.37, respectively. The associated normalized dissolution rate constant are found to $k'_{298K} = 1.2–2.4 \times 10^{-5}$ g m^{-2} d^{-1} (at pH = 0) and to $k''_{298K} = 7.8 \times 10^{-5}$ g m^{-2} d^{-1} (at pH = 14). For TUPD samples, the n and k'_{363K} values reach 0.40 and 2.8×10^{-4} g m^{-2} d^{-1} at 363 K, respectively, while for TPuPD samples, the saturation of the solution seems to be reached for shorter leaching times. From these results, the normalized dissolution rate, extrapolated to neutral medium, is evaluated to be $2.4–3.6 \times 10^{-7}$ g m^{-2} d^{-1} at room temperature and to $5.0–7.5 \times 10^{-6}$ g m^{-2} d^{-1} at 363 K.

The dependence of the reaction of dissolution on temperature was evaluated for pure TPD between 277 and 393 K and was confirmed for TUPD and TPuPD solid solutions. The activation energy (E_A)

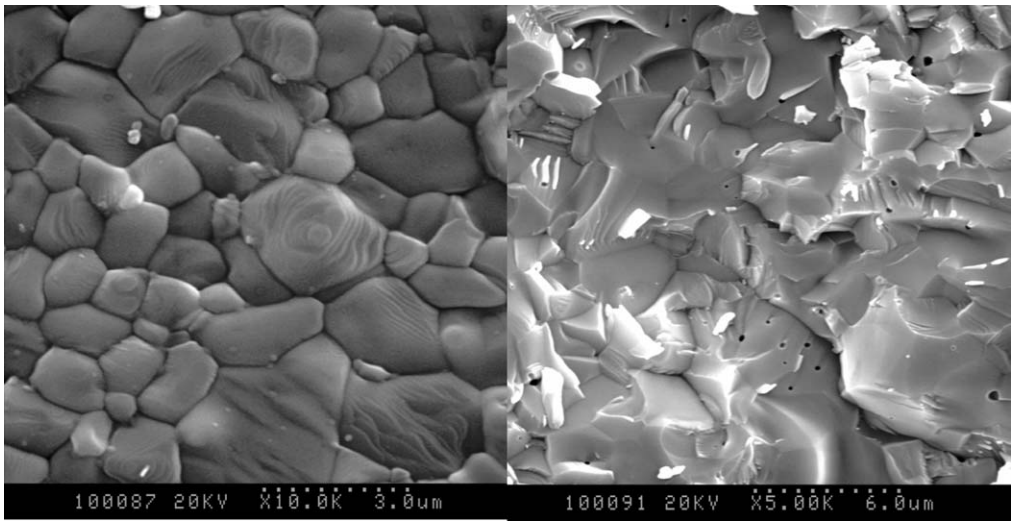

Fig. 2. SEM micrographs of surface (left) and inside (right) of sintered TUPD (24.6 wt% U).

deduced from the Arrhenius law lies between 38 and 42 kJ mol^{-1}.

The influence of the An^{IV} weight loading on the normalized dissolution rate was also examined for TUPD and TPuPD solid solutions. It appears that this parameter does not affect significantly the normalized dissolution rate for tetravalent actinides, as shown from Fig. 3. The main parameters affecting the TPD dissolution are summarized in Table 3.

When the saturation of the leachate is reached, thorium is rapidly precipitated as well-crystallized thorium phosphate hydrogenphosphate hydrate (TPHPH) [25]:

$$\log(K^{o}_{s,0}(Th_2(PO_4)_2HPO_4\cdot H_2O, \text{cryst.}, 298.15\ K) = -66.6 \pm 1.2)$$

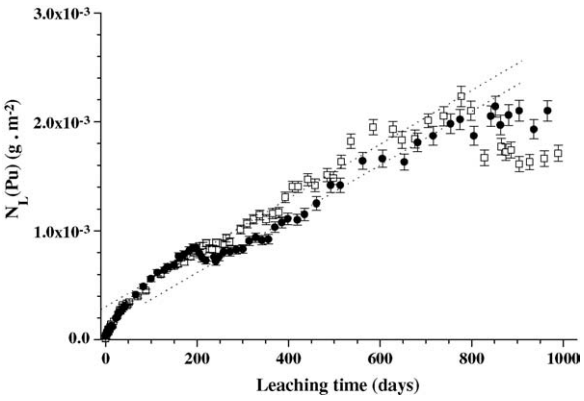

Fig. 3. Dissolution of TPuPD solid solutions (□: 16.1 wt% Pu; ●: 6.4 wt% Pu).

Table 3
Main parameters affecting the normalized dissolution rate of TPD and associated solid solutions

Parameter	
Temperature	E_A = 38–42 kJ mol^{-1}
Leachate acidity	$0.31 \le n \le 0.35$
	k'_{298K} = 1.2–2.4 × 10^{-5} g m^{-2} d^{-1} (pH = 0)
Leachate basicity	m = 0.37
	k''_{298K} = 7.8 × 10^{-5} g m^{-2} d^{-1} (pH = 14)
Ionic strength	No significant influence
Weight loading	No significant influence (U, Pu)
Redox conditions	High influence (U)
Phosphate, sulphate, chloride	Low influence
Morphology (pellet/powder)	Low influence

while uranium formed crystals of uranyl phosphate pentahydrate ($\log(K_{s,0}^{o}((UO_2)_3(PO_4)_2\ 5\ H_2O$, cryst., 298.15 K) = –55.2 ± 0.8) [26]. For the other actinides studied, the first results indicated that tetravalent plutonium forms a phosphate-based precipitate similar to TPHPH, while trivalent americium and curium are probably precipitated in a rhabdophane-type structure ($(\log(K_{s,0}^{o}(AnPO_4\cdot 0.5\ H_2O$, cryst., 298.15 K) = –27.4 ± 0.5 for americium and –29.2 ± 0.4 for curium) [27]. In these conditions, all these low-soluble neoformed phases could delay significantly the release of the radionuclides to the biosphere.

3. Monazites and brabantites

3.1. Synthesis, characterisation, and sintering

The behaviour of actinides in monazites $LnPO_4$ (monoclinic system, space group: $P2_1/n$) was already described by Kelly et al. [28]. Actinide-doped $LnPO_4$ single crystals were grown by means of a flux method. Several samples of La-monazite doped with uranium (1.7 wt%), neptunium (1.5–3 wt%), plutonium (4.3–6.0 wt%), americium (0.2 wt%) or curium (0.1–0.25 wt%) were prepared. The synthesis of La-monazite doped with americium ^{241}Am (specific activity of 2.1 × 10^7 Bq g^{-1}) was also described by Aloy et al. starting from a mixture of lanthanum and americium nitrate solutions in 1M HNO_3 and concentrated phosphoric acid [29]. The sintered samples (prepared after hot-pressing at 29.4 MPa then heating between 1173 and 1473K) exhibit an apparent density of about 84% and a rather high resistance to dissolution at 263 K in distilled water [29].

More recently, several $La_{1-x}Gd_xPO_4$ solid solutions were prepared in the monazite- or in the rhabdophane-type structure (hexagonal system, space group: $P3_121$) for several x values using three methods of preparation (direct evaporation, syntheses in closed PTFE containers on a sand bath or in autoclave). Samples of rhabdophane $La_{1-x}Gd_xPO_4\cdot n\ H_2O$ ($n \approx 0.5$) are prepared at 423 K for $x \ge 0.4$, while monazites are obtained for $x \le 0.3$. By this way, well-crystallized and single phase samples of $MPO_4\cdot n\ H_2O$ ($n \approx 0.5$–1) in the monazite (La, Ce), rhabdophane (Nd, Sm, Eu, Gd, Tb, Dy) or xenotime (Ho, Er, Tm, Yb, Lu) (tetragonal system, space group: $I4_1/amd$) forms are also prepared [30].

On the basis of the variation of the specific area versus the holding temperature and of the dilatometric studies, the sintering of these solids is found to be efficient between 1523 and 1673 K. At 1573 K, the effective relative densities of the Gd-monazite pellets prepared using a two-step procedure (pressing between 200 and 700 MPa at room temperature then heating treatment for several hours) reaches 96% of the value calculated from XRD data.

The incorporation of large amounts of tetravalent thorium or uranium was obtained in the monazite structure by the simultaneous incorporation of calcium leading to the formation of $CaTh(PO_4)_2$ and $CaU(PO_4)_2$ brabantites [5,7,31]. Nevertheless, $CaU(PO_4)_2$ was prepared as a pure phase only when firing the samples at 1473K under inert conditions. More recently, crystals of solid solutions of $La_{1-2x}U_xCa_xPO_4$ ($0 \le x \le 0.5$) were successfully prepared using hydrothermal conditions (1053 K, 200 MPa) in the presence of a Ni/NiO buffer in order to control the dioxygen fugacity and to avoid the oxidation of uranium (IV) into uranyl [5]. However, for all the samples, some crystals of $U_2(P_3O_{10})(PO_4)$ (previously known as β-UP_2O_7) [32] were coprecipitated as a minor phase. Several samples of composition $CaNp(PO_4)_2$ and $CaNp_{0.7}Pu_{0.3}(PO_4)_2$ were successfully synthesized by Tabuteau et al. using a mixture of powdered NpO_2, PuO_2, $CaCO_3$ and $(NH_4)_2HPO_4$. In these solids, both actinides are incorporated in the tetravalent state [33]. According to the results of Podor et al. [5], the formation of brabantites is driven by the ionic radius of the divalent cation, $\overline{^{IX}r(M^{II})}$, tetravalent cation, $\overline{^{IX}r(M^{IV})}$, and the average cationic radius $\overline{^{IX}r(M^{IV+II})}$ in the monazite structure under the following conditions:

$$\begin{aligned} &1.107\ \text{Å} \le \overline{^{IX}r(M^{IV+II})} \le 1.216\ \text{Å} \\ &\text{and } 1.041\ \text{Å} \le \overline{^{IX}r(M^{II})}/\overline{^{IX}r(M^{IV})} \le 1.238 \end{aligned} \quad (4)$$

3.2. Chemical durability

Only few results are available on the dissolution of monazites. In the early 1980s, Boatner et al. reported the dissolution of $La(Am)PO_4$ crystals (0.5 wt% of Am_2O_3) in distilled water at 473 K and 1.7 MPa [34]. More recently, an experimental study of the dissolution of natural monazite was developed by Oelkers et al. as a function of temperature from 323 to 503 K and for pH values ranging from 1.5 to 10. The steady state dissolution rates vary from 4×10^{-18} to 3×10^{-16} mol cm^{-2} s^{-1} (i.e. 8×10^{-7} to 6×10^{-4} g m^{-2} day^{-1}) at 343 K [35]. Several papers published by Olander et al. were also devoted to the quantitative modelling of uranium and thorium leaching from monazite in the presence of carbonate ions. The differences in the leaching properties between uranium and thorium (uranium leached more readily than thorium from monazite) persist throughout sequential leaching tests over 6 to 8 years [36–38].

We also evaluated the chemical durability of sintered samples of Gd-monazite in several acidic media between room temperature and 363 K. The low normalized dissolution rates (between 10^{-6} and 10^{-3} g m^{-2} d^{-1}) measured even in very acidic media confirms the good retention properties of this kind of matrix for the immobilisation of radionuclides and especially for trivalent actinides. Moreover, trivalent cations are generally quickly precipitated as well-crystallized neoformed phases $LnPO_4 \cdot n\ H_2O$ ($n \approx 0.5$) in the back-end of the initial dissolution ($\log(K_{s,0}^{\circ}(Gd(PO_4) \cdot 0.5\ H_2O$, cryst, 298.15 K) between –19.2 and –23.9) [30].

4. TPD/Monazite composites

4.1. Synthesis and characterisation

As previously described, pure monazites can incorporate trivalent cations, while TPD structure was initially dedicated to tetravalent actinides. In order to immobilise simultaneously tri- and tetravalent actinides in a unique material, the synthesis of TPD/monazite based composites was developed. Uranium (IV) is used as a surrogate of tetravalent plutonium or neptunium, while Gd-monazite is used to simulate the incorporation of americium or curium as well as neutron absorber in the eventuality of the plutonium storage.

Two ways of synthesis of these composite materials are considered. The first one involves the coprecipitation of precursors of both phases, starting from a mixture of concentrated hydrochloric solutions of thorium, uranium (IV), gadolinium, and concentrated phosphoric acid. The solid prepared after heating at 423 K in a closed container for 1 to 3 weeks, is centrifuged, washed with deionised water, then dried in an oven at

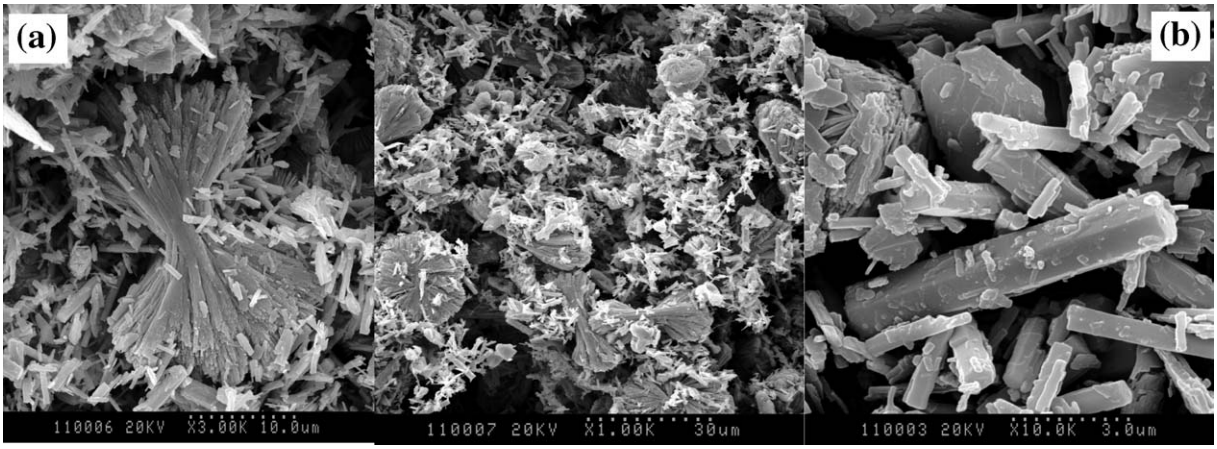

Fig. 4. Observation of precursor of TUPD/monazite composites: (**a**) TUPD precursor; (**b**) rhabdophane.

about 373 K. Its characterisation by XRD confirms that the solid is composed of a crystallized TUPD solid solutions precursor and Gd-rhabdophane. The second route of synthesis deals with the separated precipitation of both precursors. Prior to mix both solids, Gd-rhabdophane is transformed into Gd-monazite by heating between 1573 and 1773 K, then mixed mechanically to TUPD precursor. In both cases, the TUPD/monazite-based composites are obtained after heating at 1523 K for 5 to 15 h, under inert atmosphere, in order to avoid the oxidation of U(IV) into U(VI).

XRD study revealed that the solids prepared after heating at 1523 K are composed by both crystallized monazite and TUPD. The refined unit-cell parameters agree well with those reported in the literature. Moreover, no additional phase showing the reaction between both phases is demonstrated. For both ways of synthesis, EPMA and PIXE experiments show that the mole ratios and the elementary wt% are in good agreement with that expected. Nevertheless, in the case of the coprecipitation method, we observe small amounts of gadolinium in the TUPD structure (≈ 0.5 wt%) and, inversely, of thorium and uranium (IV) in the monazite (≈ 0.6 wt%). The SEM observation of low-temperature TUPD precursor/rhabdophane samples (Fig. 4) reveals the coexistence of two morphologies, Gd-rhabdophane being precipitated as needle-like crystals of about 5-μm length, while TUPD precursor crystals appear as multilayered aggregates.

4.2. Sintering

Sintering of TUPD/monazite composites was performed using a two-step procedure (uniaxial pressing at room temperature at 100–500 MPa, then heating treatment at 1523 K under inert atmosphere). For all the samples studied, the geometrical density of the pellets reaches 90 to 95% of the calculated value, which corresponds to an open porosity of about 1–6%. The densification of the pellets appears less efficient than for pure TUPD, probably due to the high porosity of monazite. BSE micrographies (Fig. 5) and EPMA experiments reveal the presence of both phases: TUPD (light phase) and monazite (dark phase). The chemical compatibility between both phases appears good at this heating temperature. However, high porosity mainly assigned to monazite is observed at the interphase.

4.3. Chemical durability

The chemical durability of TUPD/monazite composites was evaluated by performing leaching tests in several media. The good retention properties already described for pure TUPD, on the one hand, and for monazite, on the other hand, are kept in the composites materials. Indeed, the normalized dissolution rate determined at 363K from the total amount of uranium in the leachate remains very low: $2–3 \times 10^{-5}$ g m^{-2} d^{-1} and 2×10^{-6} g m^{-2} d^{-1} in 0.1M and 10^{-2}M HNO_3, respectively. They are of the same order of magnitude than that measured for pure TPD and monazite. However, large amounts of monazite in the solid seem to slightly enhance the normalized dissolution rate (for less than one order of magnitude). For all the leaching experiments, thorium and gadolinium are rapidly precipitated as neoformed thorium phosphate hydrogenphosphate hydrate and gadolinium rhabdophane, while

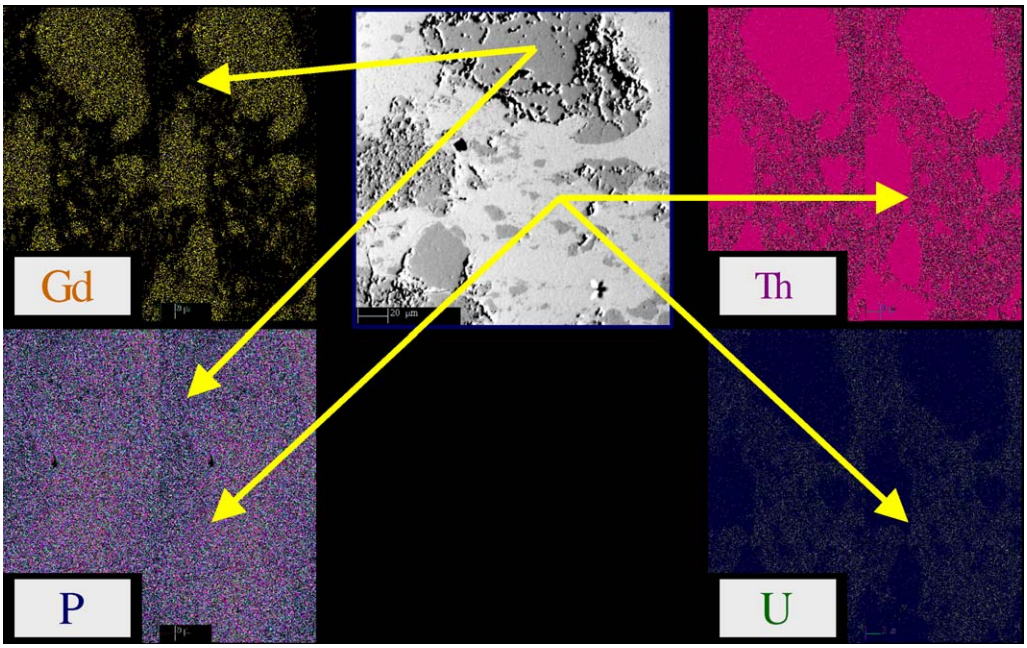

Fig. 5. X-EDS mapping of TUPD/monazite composites (dark grey: monazite; light grey: TUPD on the BSE micrograph).

uranium, which is oxidized as uranyl form, remained in the leachate.

5. Britholites

5.1. Synthesis and characterisation

Neodymium-substituted britholite $Ca_9Nd(PO_4)_5(SiO_4)F_2$ (hexagonal system, space group: $P6_3/m$) was already considered as a potential host matrix for the specific immobilisation of actinides due, for instance, to its high resistance to radiation damage [39]. This solid was first optimised for the incorporation of trivalent actinides. It was obtained from $Ca_{10}(PO_4)_6F_2$ by coupled substitution (Ca^{2+}, PO_4^{3-}) ⇌ (Nd^{3+}, SiO_4^{4-}), leading to the incorporation of trivalent cations in the structure. The incorporation of neodymium was found to occur in two steps: for $\theta \leq 1473$K, fluoro-apatite was prepared, while above this temperature, neodymium and silicate participated to the elaboration of the britholite structure [40].

We examined the incorporation of tetravalent actinides like Th, U or of Ce (as a surrogate of Pu) in the structure by coupled substitution (Nd^{3+}, PO_4^{3-}) ⇌ (An^{4+}, SiO_4^{4-}) through the preparation of $Ca_9Nd_{1-x}An^{IV}_x(PO_4)_{5-x}(SiO_4)_{1+x}F_2$ samples. This is the early beginning of the incorporation of ^{239}Pu and/or ^{238}Pu in britholite in order to evaluate the effects of α-decay in the britholite structure. Samples are prepared through dry chemistry methods from a mixture of $Nd_2O_3/CaF_2/An^{IV}O_2/Ca_2P_2O_7/SiO_2/CaCO_3$ according to the following reaction:

$$\frac{1}{4}Nd_2O_3+\frac{9}{4}Ca_2P_2O_7+\frac{7}{2}CaCO_3+CaF_2+\frac{3}{2}SiO_2 + \frac{1}{2}AnO_2 \rightarrow Ca_9Nd_{0.5}An_{0.5}(PO_4)_{4.5}(SiO_4)_{1.5}F_2+\frac{7}{2}CO_2\uparrow \quad (5)$$

In order to improve the homogeneity of the solids, the mixtures are mechanically ground in a crusher, then heated at 1673 K for 6 h under inert atmosphere in order to avoid the oxidation of U(IV) into U(VI). We showed that the incorporation of thorium and uranium is quite similar to neodymium and that a heating temperature of 1673 K is required to obtain homogeneous and single-phase compounds.

The characterisation of Th-britholites samples by XRD, SEM and EPMA for $0 \leq x \leq 1$ shows that the incorporation of this actinide in the structure is possible up to 20 wt% in the structure when considering the substitution (Nd^{3+}, PO_4^{3-}) ⇌ (Th^{4+}, SiO_4^{4-}). The

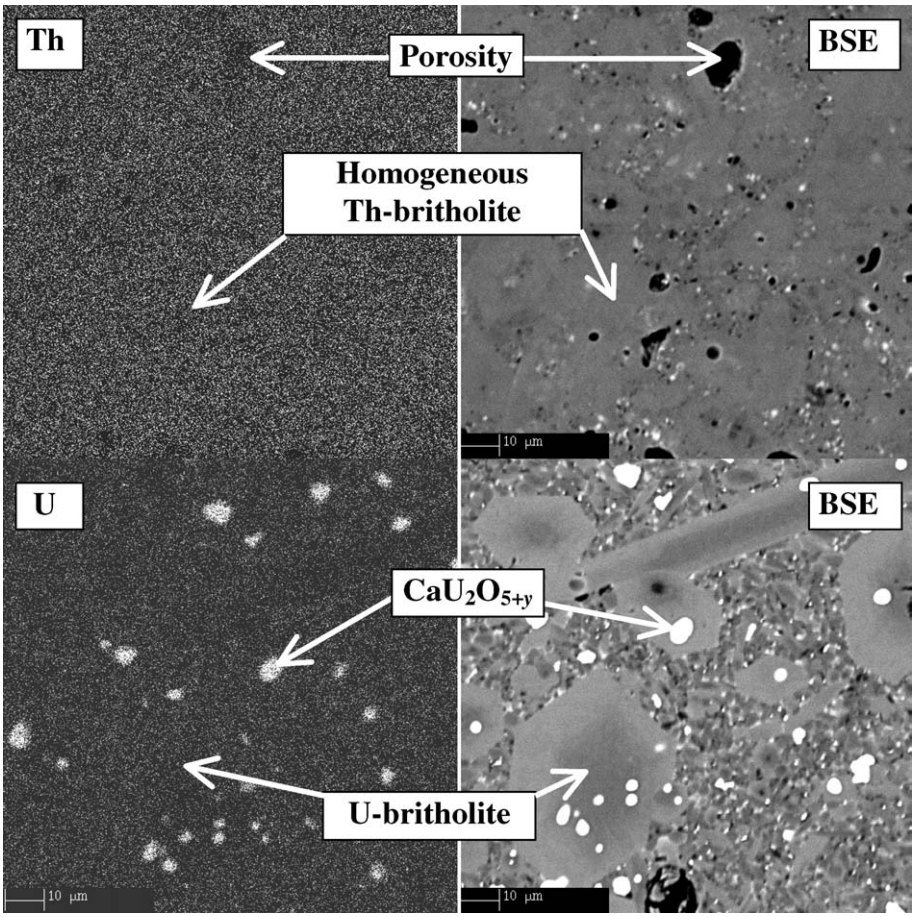

Fig. 6. X-EDS mapping of Th- and U-britholites.

samples obtained are always homogeneous and single phase as it can be seen in Fig. 6 and in Table 4. On the contrary, polyphase systems are obtained for $x \geq 0.5$ when using the $(Nd^{3+}, F^{-}) \rightleftharpoons (Th^{4+}, O^{2-})$ coupled substitution. From XRD study, the unit cell parameters and volume of Th-britholites $(Ca_9Nd_{1-x}Th_x(PO_4)_{5-x}(SiO_4)_{1+x}F_2)$ increase versus the x value according to the following equation:

$$a = 9.395(1) + 0.023(2)\ x_{Th} \quad (6)$$

$$c = 6.9002(9) + 0.012(1)\ x_{Th} \quad (7)$$

$$V = 527.2(2) + 3.4(3)\ x_{Th} \quad (8)$$

For U-britholites, the solids prepared are always composed by $Ca_9Nd_{1-x}U_x(PO_4)_{5-x}(SiO_4)_{1+x}F_2$ and calcium uranate CaU_2O_{5+y}, which shows that the incorporation is incomplete (Table 4 and Fig. 6). In most cases, only 5 wt% of uranium is introduced into the structure instead of 10 wt% expected. For sintered samples, the incorporation of uranium increases up to 7–8 wt%, while calcium uranate is mainly present at the surface of the samples [41].

Table 4
Homogeneity of $Ca_9Nd_{1-x}An_x^{IV}(PO_4)_{5-x}(SiO_4)_{1+x}F_2$ (britholite)

M(IV)	$^{VII}r_{cat.}$ (Å)	x (average)	Homogeneity
Th	1.00	0.53	Good
U	0.95	0.27	Poor, presence of CaU_2O_{5+y}
Ce	0.92	0.52	Good
Pu	0.91	ND	ND

ND: Not determined

Table 5
Refinement of the unit cell parameters of Th-, U- and Ce-britholite samples

Compound	a (Å)	c (Å)	V (Å^3)
$Ca_9Nd(PO_4)_5(SiO_4)F_2$	9.397(1)	6.905(1)	528.0(2)
$Ca_9Nd_{0.5}Th_{0.5}(PO_4)_{4.5}(SiO_4)_{1.5}F_2$	9.404(1)	6.900(1)	528.5(2)
$Ca_9Nd_{0.5}U_{0.5}(PO_4)_{4.5}(SiO_4)_{1.5}F_2$	9.3917(7)	6.8950(8)	526.7(1)
$Ca_9Nd_{0.5}Ce_{0.5}(PO_4)_{4.5}(SiO_4)_{1.5}F_2$	9.3994(9)	6.905(1)	528.3(2)

The incorporation of Pu(IV) was studied using Ce(IV) as a surrogate ($r_{Pu}^{4+} = 0.91$ Å and $r_{Ce}^{4+} = 0.92$ Å in the seven-fold coordination). Nevertheless, during the synthesis of Ce-britholites, Ce(IV) is partly reduced in Ce(III) when heating at high temperature. It is confirmed by the values of the unit cell parameters (Table 5), which should be smaller in the case of pure Ce(IV)-britholites compared to Th-britholites.

5.2. Sintering

Grinding of the raw powder $Ca_9Nd(PO_4)_5(SiO_4)F_2$ by attrition allows us to increase the surface area from 0.2 m^2 g^{-1} up to 23.3 m^2 g^{-1} and to decrease the sintering temperature from 1873 to 1593 K with an increase of the relative density up to 97% of the calculated value (1748 K, 6 h).

The influence of CaF_2 on the sinterability of monosilicated fluor-apatite was studied by comparison between powder prepared using classical route and that prepared from NdF_3, which contains 0.5 mol of CaF_2:

$$NdF_3 + \frac{5}{2}\,Ca_2P_2O_7 + \frac{9}{2}\,CaCO_3 + SiO_2 \rightarrow Ca_9Nd(PO_4)_5(SiO_4)F_2 + \frac{1}{2}\,CaF_2 + \frac{9}{2}\,CO_2\uparrow \quad (9)$$

Sintering of this powder at 1373 K for 4 h leads to a density of 99.5% of calculated value. The addition of CaF_2 in this powder leads to a decrease of the sintering temperature to 1373 K with a relative density of 94% [42]. Complementary studies on sintering of britholites doped with tetravalent actinides like Th, U or with Ce are now under progress in order to evaluate the influence of their composition on sinterability.

5.3. Chemical durability

Britholites dissolution rates were measured versus pH (between 4 and 6 at 363 K) and temperature (298–473 K). All the experiments were carried out in flow-through reactors for the dissolution-rate law determination. The effects of several synthesis parameters, sintering type (natural or uniaxial pressing) and initial neodymium reagent (Nd_2O_3 or NdF_3) were also evaluated by soxhlet leaching tests (distilled water at 373 K). For all the experiments including soxhlet tests, normalized dissolution rates are determined from the calcium amount in the leachate, since fluoride is preferentially released in solution due to its structural localization in the apatite lattice channels, and neodymium (as trivalent actinide surrogate) quickly precipitates with phosphates to form the hydrated rhabdophane $Nd(PO_4)\cdot 0.5\,H_2O$ (Fig. 7) in most of our experimental conditions. No significant effect of synthesis parameter on dissolution rates is detected. The influence of pH (Fig. 8) on the normalized dissolution rate can be expressed by:

$$\log(R_L) = 4.04 - 1.07\ \text{pH}\ \ (\text{at}\ 363\ \text{K}) \quad (10)$$

The apparent activation energy (E_A) deduced from an Arrhenius law is 30 kJ mol^{-1} for pH = 4.1. Normalized dissolution rates of britholites, pH dependence and E_A are consistent with recent data obtained by Guidry et al. [43], suggesting the same dissolution

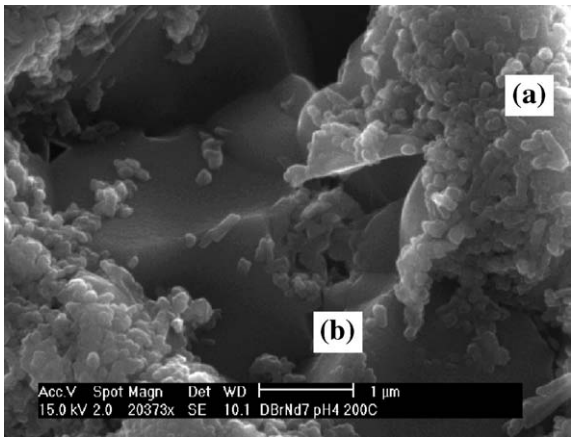

Fig. 7. SEM micrograph of neoformed $Nd(PO_4)\cdot 0.5\,H_2O$ (**a**) precipitated at the surface of residual britholite (**b**).

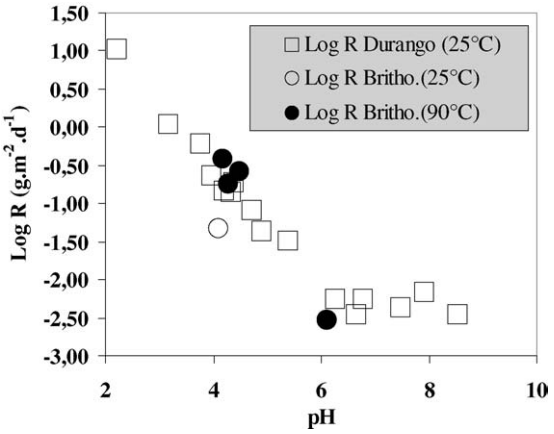

Fig. 8. pH effect on the britholite and natural Durango apatite dissolution rates.

mechanism and long-term behaviour for synthetic and natural solids (Fig. 8).

When thermodynamic equilibriums are reached, actinides concentrations are controlled in the leachate by the low solubility of secondary phosphate-based neoformed phase. The behaviour of tetravalent actinides through the study of the chemical durability of Th-, U- and Ce-britholites during leaching tests is now under progress.

6. Conclusions

On the basis of all the properties studied up to now, several phosphate materials appear as good candidates for the immobilisation of tetravalent actinides (TPD, brabantites, britholites and TPD/monazite composites), like uranium, neptunium, plutonium, and certainly protactinium (IV) or trivalent actinides (monazites, britholites and TPD/monazite composites) such as americium and curium. Indeed, the preparation of solids doped with actinides leads, in most cases, to the preparation of homogeneous and single-phase compounds through wet and/or dry chemical methods. These materials exhibit rather good sintering properties: for each kind of solid, dense pellets can be prepared using a two-step procedure involving uniaxial pressing at room temperature then heating at high temperature even though for monazite and TPD/monazite composites, a decrease of the open porosity is now required in order to decrease the specific surface area of the final solid.

The chemical durability of these solids is found to be rather high, even in aggressive media. Moreover, phosphate-based phases formed in the back end of the dissolution of the initial solid are poorly soluble, which should delay significantly the release of tri- and tetravalent actinides in the field of an underground repository. The resistance of these materials to radiation damages are now under study by using external irradiations with α particles or heavy ions or by synthesising samples doped with short half time radionuclides such as ^{238}Pu ($T_{1/2}$ = 87.7 yr). The main results of the resistance of TPD to radiation damages as well as its consequences on the dissolution will be published soon.

Acknowledgements

This work was performed with the support of French Research Group NOMADE (*NOuveaux MAtériaux pour les DÉchets*: CNRS/CEA/EDF/COGEMA). The authors would like to thank Dr Renaud Podor and Alain Kohler from LCSM (university of Nancy I, France) for performing the SEM observations and the EPMA experiments.

References

[1] R. Bros, J. Carpena, V. Sere, A. Beltritti, Radiochim, Acta 74 (1996) 277.
[2] J. Carpena, F. Audubert, D. Bernache, L. Boyer, B. Donazzon, J.-L. Lacout, N. Senamaud, in: I.G. McKinley, C. McCombie (Eds.), Scientific Basis for Nuclear Waste Management, XXI, 1998, p. 543.
[3] L.A. Boatner, B.C. Sales, in: W. Lutze, R.C. Ewing (Eds.), Radioactive Waste Forms for the Future, North-Holland Physics Publishing, Amsterdam, 1998, p. 495.
[4] A. Meldrum, L.A. Boatner, W.J. Weber, R.C. Ewing, Geochim. Cosmochim. Acta 62 (1998) 2509.
[5] R. Podor, M. Cuney, Am. Miner. 82 (1997) 765.
[6] R. Podor, M. Cuney, C. Nguyen Trung, Am. Miner. 80 (1995) 1261.
[7] J.-M. Montel, J.-L. Devidal, D. Avignant, Chem. Geol. 191 (2002) 89.
[8] H.T. Hawkins, B.E. Scheetz, G.D. Guthrie, Chem. Mater. 11 (1999) 2851.
[9] A.I. Orlova, Y.F. Volkov, R.F. Melkaya, L.Y. Matserova, I.A. Kulikov, V.A. Alferov, Radiokhimimiya 36 (1994) 322.
[10] L. Bois, M.J. Guittet, F. Carrot, P. Trocellier, M. Gautier-Soyer, J. Nucl. Mater. 297 (2001) 129.

[11] P. Bénard, V. Brandel, N. Dacheux, S. Jaulmes, S. Launay, C. Lindecker, M. Genet, D. Louër, M. Quarton, Chem. Mater. 8 (1996) 181.
[12] J. Carpena, in: P. Van den Haute, F. de Corte (Eds.), Advances in Fission Track Geochronology, Kluwer Academic Press, 1998, p. 81.
[13] P. Benard, D. Louër, N. Dacheux, V. Brandel, M. Genet, Chem. Mater. 6 (1994) 1049.
[14] P. Benard, D. Louër, N. Dacheux, V. Brandel, M. Genet, An. Quim. Int. Ed. 92 (1996) 79.
[15] V. Brandel, N. Dacheux, M. Genet, J. Solid State Chem. 121 (1996) 467.
[16] V. Brandel, N. Dacheux, J. Rousselle, M. Genet, C. R. Chimie 5 (2002) 599.
[17] V. Brandel, N. Dacheux, M. Genet, Radiokhimiyia 43 (2001) 16.
[18] R.D. Shanon, Acta. Crystallogr. 5 (1975) 186.
[19] V. Brandel, N. Dacheux, E. Pichot, M. Genet, J. Emery, J.-Y. Buzare, R. Podor, Chem. Mater. 10 (1998) 345.
[20] N. Dacheux, R. Podor, B. Chassigneux, V. Brandel, M. Genet, J. Alloys Compds 271 (1998) 236.
[21] N. Dacheux, R.R. Podor, V. Brandel, M. Genet, J. Nucl. Mater. 252 (1998) 179.
[22] N. Dacheux, A.C. Thomas, V. Brandel, M. Genet, J. Nucl. Mater. 257 (1998) 108.
[23] A.-C. Thomas, Étude de la dissolution du phosphate diphosphate de thorium : aspect cinétique, aspect thermodynamique, thesis, University Paris-11, Orsay, France, 2000, IPNO-T-00.09.
[24] N. Dacheux, B. Chassigneux, V. Brandel, P. Le Coustumer, M. Genet, G. Cizeron, Chem. Mater. 14 (2002) 2953.
[25] A.-C. Thomas, N. Dacheux, P. Le Coustumer, V. Brandel, M. Genet, J. Nucl. Mater. 281 (2000) 91.
[26] A.-C. Thomas, N. Dacheux, V. Brandel, P. Le Coustumer, M. Genet, J. Nucl. Mater. 295 (2001) 249.
[27] A.-C. Robisson, N. Dacheux, J. Aupiais, J. Nucl. Mater. 306 (2002) 134.
[28] K.L. Kelly, G.W. Beall, J.P. Young, L.A. Boatner, in: J.G. Moore (Ed.), Scientific Basis for Nuclear Waste Management, Vol. 3, 1980, p. 189.
[29] A.S. Aloy, E.N. Kovarskaya, T.I. Kolsova, S.E. Samoylov, S.I. Rovnyi, G.M. Medvedev, L.J. Jardine, Proc. 10th Int. Ceramics Congress2002, CD-Rom.
[30] O. Terra, N. Clavier, N. Dacheux, R. Podor, New J. Chem. 27 (2003) 957.
[31] D.D. Davis, E.R. Vance, G.J. McCarthy, in: J.G. Moore (Ed.), Scientific Basis for Nuclear Waste Management, Vol. 3, 1980, p. 197.
[32] R. Podor, M. François, N. Dacheux, J. Solid State Chem. 172 (2003) 66.
[33] A. Tabuteau, M. Pages, J. Livet, C. Musikas, J. Mater. Sci. Lett. 7 (1988) 1315.
[34] L.A. Boatner, G.W. Beall, M.M. Abraham, C.B. Finch, P.G. Huray, M. Rappaz, in: C.J.M. Northrup Jr (Ed.), Scientific Basis for Nuclear Waste Management, Vol. 2, 1981, p. 289.
[35] E.H. Oelkers, F. Poitrasson, Chem. Geol. 191 (2002) 73.
[36] Y. Eyal, D.R. Olander, Geochim. Cosmochim. Acta 54 (1990) 1867.
[37] D.R. Olander, Y. Eyal, Geochim. Cosmochim. Acta 54 (1990) 1879.
[38] D.R. Olander, Y. Eyal, Geochim. Cosmochim. Acta 54 (1990) 1889.
[39] J. Carpena, L. Boyer, M. Fialin, J.-R. Kiénast, J.-L. Lacout, C. R. Acad. Sci. Paris, Ser. IIa 333 (2001) 373.
[40] L. Boyer, Synthèse et caractérisation d'apatites phosphosilicatées aux terres rares : implication au nucléaire, thesis, INP, Toulouse, France, 1998.
[41] O. Terra, N. Dacheux, F. Audubert, C. Guy (to be published).
[42] F. Audubert, D. Bernache-Assollant, in: P. Vincenzini (Ed.), Advances in Science and Technology – Proc. 10th Int. Ceramics Congress – CIMTEC 2002, 2002, Part B, 31, p. 61.
[43] M.W. Guidry, F.T. Mackenzie, Geochim. Cosmochim. Acta 67 (2003) 2949.